

Investigation of a Ball Screw Feed Drive System Based on Dynamic Modeling for Motion Control

Yi-Cheng Huang^{*}, Xiang-Yuan Chen

Department of Mechatronics Engineering, National Changhua University of Education,
Changhua, Taiwan.

Received 01 February 2016; received in revised form 28 April 2016; accepted 02 May 2016

Abstract

This paper examines the frequency response relationship between the ball screw nut preload, ball screw torsional stiffness variations and table mass effect for a single-axis feed drive system. Identification for the frequency response of an industrial ball screw drive system is very important for the precision motion when the vibration modes of the system are critical for controller design. In this study, there is translation and rotation modes of a ball screw feed drive system when positioning table is actuated by a servo motor. A lumped dynamic model to study the ball nut preload variation and torsional stiffness of the ball screw drive system is derived first. The mathematical modeling and numerical simulation provide the information of peak frequency response as the different levels of ball nut preload, ball screw torsional stiffness and table mass. The trend of increasing preload will indicate the abrupt peak change in frequency response spectrum analysis in some mode shapes. This study provides an approach to investigate the dynamic frequency response of a ball screw drive system, which provides significant information for better control performance when precise motion control is concerned.

Keywords: Ball nut preload, ball screw drive system, dynamic modeling

1. Introduction

Precision computer numerical control (CNC) machines are widely used in modern industry for mass production. The ball screws are widely applied in the linear actuators of machinery and equipment because of the high efficiency, less backlash, easy lubrication, and easy maintenance. Since ball screw play a significant role in con-

verting rotary motion into linear motion Pre-loading is effective to eliminate backlash and increase the stiffness of ball screw for precision motion concerns. The dynamic frequency responses of the feed drive system depends on the stiffness combinations of the ball screw, ball nut, fixed support bearings, the flexible coupler and the stiffness between the ball screw and the working table. Such frequency response results from the axial mode shapes and torsional mode shape of the ball screw drive system when it is actuated by servo motor. Each mode shape affects and determines the motion control frequency response bandwidth when the control speed is limited and becomes a critical issue. The working table mass and the bolt stiffness between the machine bed base and attached ground floor also plays an important role for the frequency response when the vibration mode of the CNC machine is concerned with precision accuracy.

As in intelligent control field, the control signals that fed into the controlled plant are based on the feedback control error that should be learnable. Therefore, some control efforts [1-2] are focused the design of the bandwidth of the filter that can filter out the un-learnable errors contents and can be get back to control system for bettering control history. Since the bandwidth of controlled system determines the motion speed response and its performance. The lumped dynamic model derivation is significant in determining the bandwidth for motion control law that can be used for controller design. Since such frequency contents of compensated error are suggested to be within the bandwidth when control signals are actuating. This paper will derive the dynamic model of the ball screw feed drive system first and examine the relationship between the ball screw preload variation, ball screw torsional stiffness and effect of table mass.

* Corresponding author, Email: ychuang@cc.ncue.edu.tw

Simulation results will unveil the frequency response of the translational and torsional peak modes. Numerical simulation shows stable convergence by using hybrid particle swarm optimization of iterative learning control [2] on this developed ball screw drive system.

2. Mathematical Model and Numerical Simulation

2.1. Dynamic Model of the Ball Screw Drive System

To model the feed drive system, this paper set different stiffness of the ball nut stiffness for different preload between the ball screw shaft and the ball nut. The presetting preload value can be deployed by inserting different ball size for single ball nut design or using disk spring that applied to the ball screw when double ball nut is the preference. Fig. 1 shows the picture of the in-lab single-axis feed drive platform. To analyze the dynamic characteristic of the ball screw system under different preload and varying table mass, the feed drive system is modeled by a lumped parameter system shown in Fig. 2. Fig. 2 is the schematic illustration for the single-axis ball screw feed drive system. In general, mechanical systems have three passive linear components. The spring and the mass are energy-storage elements, while the viscous damper is the dissipated energy. Both of the rotational and translation mechanical system modeled below are actuated by the servo motor torque, indicated as T . As the same derivation in [3], the overall stiffness of a ball screw feed drive system can be determined by the stiffness of the ball screw itself, which is comprised of the ball screw shaft, the ball nut, supporting bearings of the ball screw, and the stiffness between the ball screw and the working table.

$$J_m \times \ddot{\theta}_m + Q_m \times \dot{\theta}_m + K_g \times (\theta_m - \theta_b) = T \quad (1)$$

$$J_b \times \ddot{\theta}_m + Q_m \times \dot{\theta}_b + R \times [K_n \times (R \times \theta_b + X_b - X_t)] = K_g \times (\theta_m - \theta_b) \quad (2)$$

$$M_b \times \ddot{X}_b + B_b \times (\dot{X}_b - 0) + K_e \times (X_b - 0) + K_n \times (R \times \theta_b + X_b - X_t) = 0 \quad (3)$$

$$M_t \times \ddot{X}_t + B_t \times (\dot{X}_t - 0) = K_n(R\theta_b + X_b - X_t) \quad (4)$$

Rearranging Eqs (1)-(4), we have

$$\begin{bmatrix} M_t & 0 & 0 & 0 \\ 0 & M_b & 0 & 0 \\ 0 & 0 & J_b & 0 \\ 0 & 0 & 0 & J_m \end{bmatrix} \times \begin{bmatrix} \ddot{X}_t \\ \ddot{X}_b \\ \ddot{\theta}_b \\ \ddot{\theta}_m \end{bmatrix} + \begin{bmatrix} B_t & 0 & 0 & 0 \\ 0 & B_b & 0 & 0 \\ 0 & 0 & Q_b & 0 \\ 0 & 0 & 0 & Q_m \end{bmatrix} \times \begin{bmatrix} \dot{X}_t \\ \dot{X}_b \\ \dot{\theta}_b \\ \dot{\theta}_m \end{bmatrix} + \begin{bmatrix} K_n & -K_n & -K_n R & 0 \\ -K_n & K_e + K_n & K_n R & 0 \\ -K_n R & K_n R & K_g + K_n R^2 & -K_g \\ 0 & 0 & -K_g & K_g \end{bmatrix} \times \begin{bmatrix} X_t \\ X_b \\ \theta_b \\ \theta_m \end{bmatrix} = \begin{bmatrix} 0 \\ 0 \\ 0 \\ T \end{bmatrix} \quad (5)$$

where the stiffness matrix is different from [3].

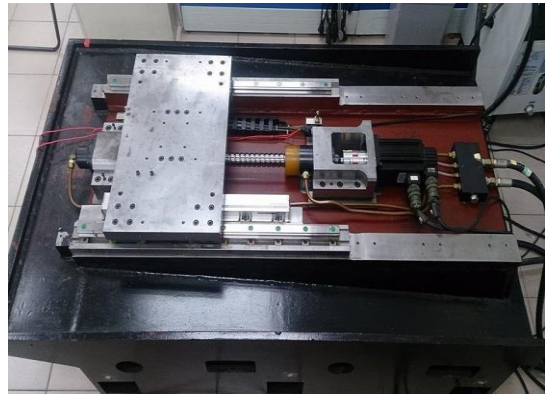


Fig. 1 The in-house single axis platform

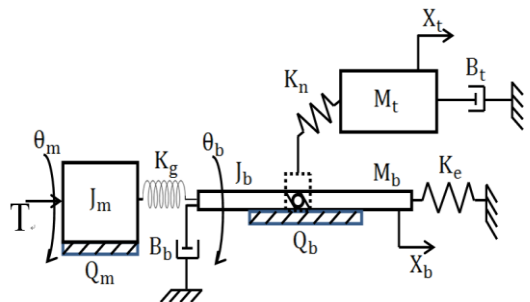


Fig. 2 Illustration for the schematic diagram of the single-axis lumped parameters ball screw drive system

2.2. Numerical Simulation

Table 1 list the simulated parameters and associated values used in Eqs (1)-(4). The dynamic equation of the single-axis feed drive system model with varied preload and table mass can be expressed in a compact form:

$$[M]\{\ddot{u}\} + [C]\{\dot{u}\} + [K]\{u\} = f \quad (6)$$

where [M], [C], and [K] are the 4x4 square matrices, referred as the mass (or the moment of inertia), the viscous damping, and the stiffness matrices, respectively. {u} represents a four degree of freedom model. It consists with the X_t , X_b , θ_b , and θ_m for the displacement of the working table, axial displacement of the ball screw, rotation angle of the ball screw, and the rotation angle of the motor, respectively.

Table 1 Important parameters of ball screw drive system

Parameters	value
working table mass (Mt)	47.09Kg
ball screw mass (Mb)	9Kg
inertia moment of the motor (Jm)	$4.45 \times 10^{-4} \text{kgm}^2$
inertia moment of the ball screw (Jb)	$1.3 \times 10^{-3} \text{kgm}^2$
equivalent axial stiffness of ball screw shaft (Ke)	$1.8663 \times 10^7 \text{N/m}$
stiffness of the ball nut (Kn)	$2.3345 \times 10^8 \text{N/m}$
torsional stiffness of the ball screw (Kg)	$3.49 \times 10^8 \text{N/m}$
viscous damping coefficient of the guide way of the working table (Bt)	10N s/m
viscous damping coefficient of the supporting bearing of the ball screw (Bb)	10N s/m
rotational viscous damping coefficient of the motor (Qm)	0N ms
rotational viscous damping coefficient of the support bearing of ball screw (Qb)	0N ms
angle conversion axial displacement of the constant (R)	0.0025
motor torque (T)	$1.8 \times 10^{-3} \text{Nm/s}^2$
displacement of the working table (Xt)	State Variable (m)
axial displacement of the ball screw (Xb)	State Variable (m)
rotation angle of the motor (θ_m)	State Variable (rad)
rotation angle of the ball screw (θ_b)	State Variable (rad)

The homogeneous solution of Eqs (5) represents the transient response of the lumped system whereas the forcing function of applied motor torque renders the table positioning. Homogeneous solution of the Equation (2.1.5) results in four eigenvectors V1, V2, V3, and V4 associated with each eigenvalue ($\lambda = \omega^2$) of 3.2124×10^4 , 3.3322×10^6 , 1.0699×10^{11} , $3.421 \times 10^7 \text{rad}^2/\text{s}^2$.

$$\begin{aligned}
 V1 &= \begin{Bmatrix} -0.7299 \\ -0.6836 \\ 0 \\ 0 \end{Bmatrix} & V2 &= \begin{Bmatrix} 0.1762 \\ -0.9844 \\ 0 \\ 0 \end{Bmatrix} \\
 V3 &= \begin{Bmatrix} 0 \\ 0 \\ 0.9482 \\ -0.3176 \end{Bmatrix} & V4 &= \begin{Bmatrix} 0 \\ 0 \\ 0.7067 \\ 0.7076 \end{Bmatrix}
 \end{aligned} \quad (7)$$

The four eigenvectors corresponding to the Eigen frequencies of 28.52 Hz, 290.52 Hz, 52059 Hz, 930.9 Hz w is calculated by 2% of the rated dynamic load. These eigenvectors represent the mode shapes of the ball screw feed drive system. The first three significant Eigen frequencies are related to the three resonant frequencies. The first and second modes are from the axial vibration. The third mode is from the torsional vibration. In Eqs (7), the first mode of the working table and the balls screw is moving in phase while the second mode is moving out of phase. Fig. 3 shows the bode plot of the dynamic system based on different K_n values. The preload variation is simulated from 2%, 4%, 6%, 8% to 10% of the rated dynamic loading of the ball screw.

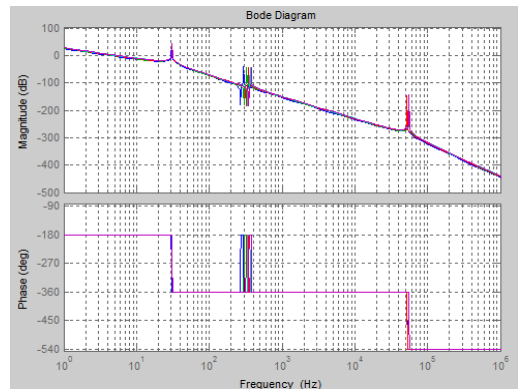


Fig. 3 Bode plot of the ball screw drive system based on the preload value of 2% (blue), 4% (green), 6% (red), 8% (cyan) and 10% (purple) of the rated dynamic loading

Enlargement of the first, second and third modes of the bode plot, the three frequencies are ranging from 30.5 Hz to 30.8 Hz, 294 Hz to 380 Hz and 52000 Hz to 55000 Hz respectively. It is obvious that the second translational mode will be affected more than the first mode when the ball nut preload is varying. The solution of the fourth mode is about 930 Hz, the contribution of this mode is not significant even though the preload is varied.

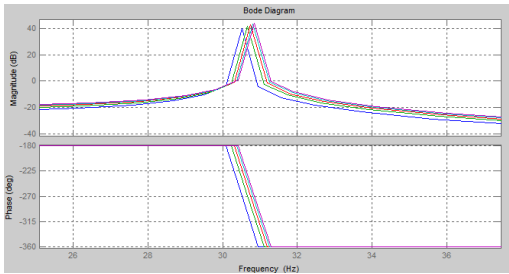


Fig. 4 The enlargement of the first mode of the bode plot in Fig. 3 based on different ball nut stiffness

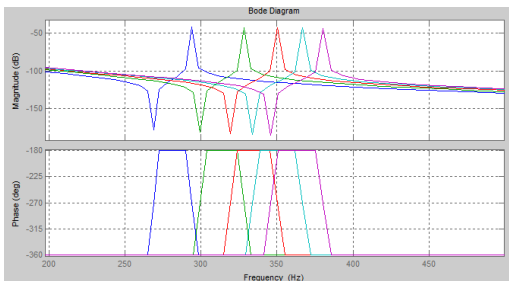


Fig. 5 The enlargement of the second mode of the bode plot in Fig. 3 based on different ball but stiffness

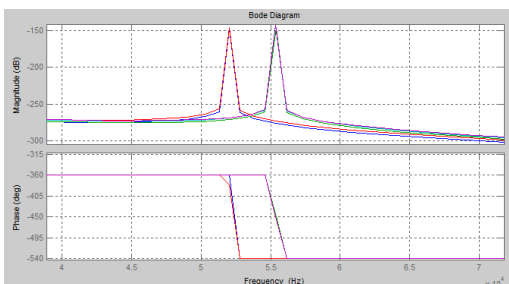


Fig. 6 The enlargement of the third mode of bode plot in Fig. 3 based on different ball nut stiffness

As stated, the third eigenvector indicates the torsional vibration. Since the servo motor drives the ball screw through a coupler providing damping and stiffness. The torsional stiffness of

the ball screw is investigated by calculating K_g by $\pi d_r^4 G / 32L$. Fig. 7 shows the variations of K_g in the range of $\pm 10\%$. As shown, the third mode demonstrates large frequency shift with increasing the torsional stiffness of the ball screw. Fig. 8 indicates the frequency shift is range from 50700 Hz to 58000 Hz, while the first and second modes are not changed noticeably.

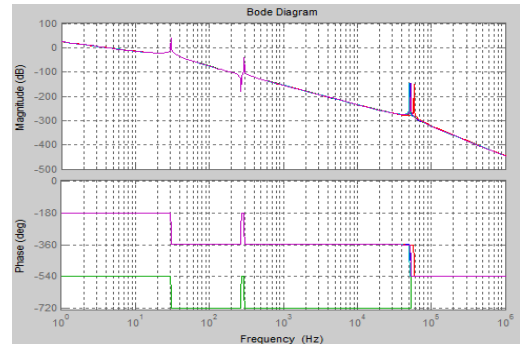


Fig. 7 Bode plot of the ball screw torsional stiffness 100% (blue), 105% (green), 110% (red), 95% (cyan), 90% (purple)

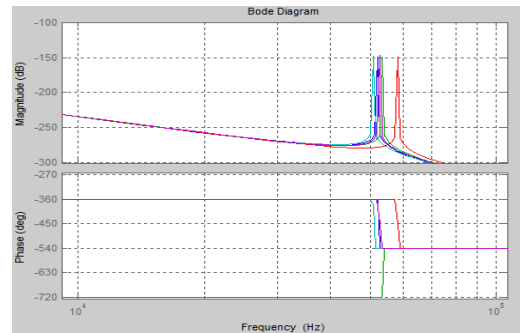


Fig. 8 The enlargement of the torsional mode of the bode plot in Fig. 7 based on different ball screw torsional stiffness

Figs. 9-11 detail the effect of the table mass. The characteristic frequency shifts from the 24Hz to 30.5Hz when the table mass increases from 47.09 kg to 94.18 kg. As predicted, the table mass preserves the effect on the first bandwidth in the translational mode and some effect on the second mode. Increasing table mass does not affect the bandwidth of the third torsional mode. Fig. 12 shows the numerical simulation plot of the convergence error when the ball screw drive system is controlled by hybrid particle swarm optimization for the dynamic bandwidth tuning of an iterative learning control.

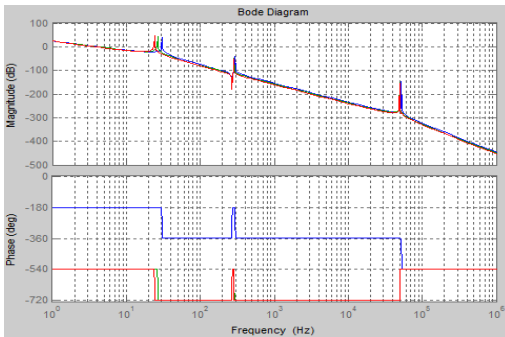


Fig. 9 Bode plot of the working table mass 47.09Kg(blue), 70.63Kg(green), 94.18Kg(red)

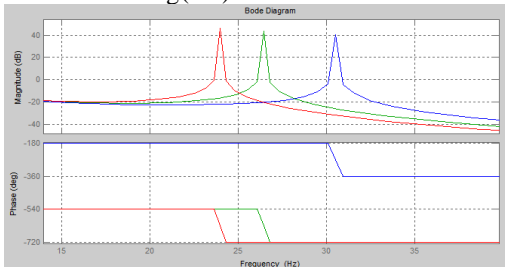


Fig. 10 The enlargement of the first mode of the bode plot in Fig. 9 based on different working table mass

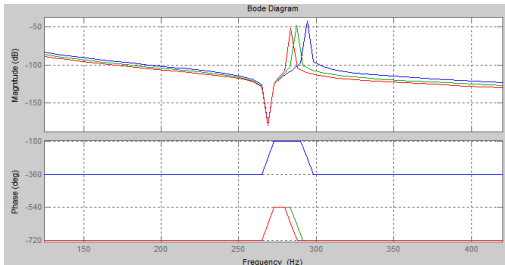


Fig. 11 The enlargement of the second mode of the bode plot in Fig. 9 based on different working table mass

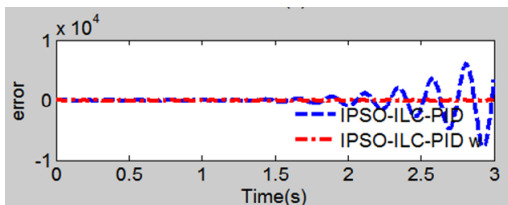


Fig. 12 Plot of a convergence error of the numerical simulation by using HPSO-ILC [2] for ball screw drive system

3. Conclusions

A lumped dynamic model for describing different ball nut preload level, ball screw torsional stiffness and the table mass effects of the ball screw feed drive system is derived and numerically simulated. Based on the different percent of the preload and table mass, the frequency spectrum analysis of the numerical simulation provides the limits and constraints of bandwidth tuning for motion control applications. The preload variation can be diagnosed by the peak frequency change and the magnitude of the peak frequency in a specific frequency range when the axial mode or the torsional mode is excited. The derivation and numerical simulation results of the lumped dynamic model provides significant information in determining the zero phase bandwidth tuning. Application of a hybrid particle swarm optimization iterative learning control law deploys successfully when the frequency contents of the compensated error was constrained in every control actuation.

Acknowledgement

This work was supported by MOST Grant 104-2221-E-018-015 for which the authors are very much grateful.

References

- [1] M. S. Tsai, C. L. Yen, and H. T. Yau, "Integration of an empirical mode decomposition algorithm with iterative learning control for high-precision machining," *IEEE/ASME Transaction on Mechatronic*, vol. 18, no. 3, pp. 878-886, 2013.
- [2] Y. C. Huang, Y. W. Su, and P. C. Chuo, "Iterative learning control bandwidth tuning using the particle swarm optimization technique for high precision motion," *Microsystem Technologies*. DOI: 10.1007/s00542-015-2649-6, 2015.
- [3] G. H. Feng and Y. L. Pan, "Investigation of ball screw preload variation based on dynamic modeling of a preload adjustable feed-drive system and spectrum analysis of ball-nuts sensed vibration signals," *International Journal of Machine Tools & Manufacture*, vol. 52, no. 1, pp. 85-96, 2012.